Kapitza resistance and thermal conductivity of Kapton in superfluid helium

B. Baudouy
CEA-Saclay, DSM/DAPNIA/SACM, 91191 Gif-sur-Yvette Cedex, France

Abstract

We have determined simultaneously the Kapitza resistance, R_k, and the thermal conductivity, κ, of Kapton HN sheets at superfluid helium temperature in the range of 1.4 – 2.0 K. Five sheets of Kapton with varying thickness from 14 µm to 130 µm, have been tested. Steady-state measurement of the temperature difference across each sheet as a function of heat flux is achieved. For small temperature difference (10 to 30 mK) and heat flux density smaller than 30 Wm^{-2}, the total thermal resistance of the sheet is determined as a function of sheet thickness and bath temperature. Our method determines with good accuracy the Kapitza resistance, $R_K=(10540\pm444)\ T^{-3}\ \times10^{-6}\ Km^2W^{-1}$, and the thermal conductivity, $\kappa=[(2.28\pm0.54)+(2.40\pm0.32)\times T\ ]\times\ 10^{-3}\ Wm^{-1}K^{-1}$. Result obtained for the thermal conductivity is in good agreement with data found in literature and the Kapitza resistance's evolution with temperature follows the theoretical cubic law.

Keywords: Electrical insulation (A); He II (B); Heat transfer (C)

Nomenclature

A	Total cross section (m^2)
ℓ	Thickness (m)
n	Exponent
Q	Heat flux (W)
R	Thermal resistance (Km^2W^{-1})
$\Delta T=T_i-T_b$	Total temperature difference (K)
T_1, T_2	Boundary temperatures due to Kapitza resistance (K)

Greek Letters

α	Kapitza coefficient ($Wm^{-2}K^{-n}$)
κ	Average thermal conductivity ($Wm^{-1}K^{-1}$)
σ	1 standard deviation from the mean value

Subscripts

b	Cryostat bath
cap	Capillary
κ	Conduction
i	Inner bath
K	Kapitza
s	Sample
sup	Support

1 Introduction

In recent years, significant interest has been shown in the thermal properties of amorphous polymers at low temperatures. Such polymers, like Kapton, exhibit good mechanical, chemical, and electrical

properties. Therefore, they are used in many cryogenic applications such as thermal and electrical insulation for superconducting magnet winding, as key components for cryogenic target or space applications, and for low temperature heat exchanger. Kapton, a registered trademark of the Dupont Company, is one of the most frequently used of such kind. For all these cryogenics applications an accurate design is required and thus the knowledge of the thermal properties of such material, such as the thermal conductivity and the thermal resistance, dominated by the Kapitza resistance, at the solid-He II interface is essential. Because the thermal conductivity and the Kapitza resistance of Kapton at superfluid temperature have not been studied extensively whereas its wide use, we have determined the thermal conductivity and the Kapitza resistance of Kapton HN sheets in the temperature range of 1.4 K to 2.0 K.

The thermal conductivity of Kapton, κ, at low temperatures has been recently measured by several groups [1-3]. Essentially, two methods are used based on steady-state heat transfer, namely the stack method and the direct method. The most popular method is to stack-up layers of Kapton tapes bonded together either with epoxy resin or with contact grease. Here, to evaluate κ, the thermal conductivity of the epoxy resin and thus the thermal resistance between the Kapton tapes and the resin has to be known. Barucci *et al.* use the direct method, where κ is determined from a measurement on a single layer of material (125 μm) [4]. The Kapton sheet is glued onto two copper disks forming a cylindrical configuration. They applied a heat flux to the sheet and measured a subsequent temperature gradient across the sample on the copper disks. This approach reduces the uncertainty arising from the contact resistance. Their findings will be compared to our results in the discussion section.

To the best of our knowledge, there is only one group, Nacher *et al.*, that published data on Kapitza resistance at sub-Kelvin temperatures on unspecified type of Kapton [5]. The principle of their experiment is similar to that used in this study: Kapton sheets separate two helium baths, one is heated and the other is temperature controlled. They measured temperature difference across the sheets as a function of heat flux neglecting conduction through the Kapton. They have determined the Kapitza resistance in the temperature range of 30–150 mK on 8 and 12 μm thick Kapton sheets. Our method is similar except that we measure temperature difference across sheets having different thickness to determine simultaneously Kapitza resistance term and the conduction term.

2 Experimental set-up

Two 100-mm diameter sample sheets are fixed over 20 mm of their diameter by Scotch-Weld™ DP190 epoxy resin and clamped with two stainless steel flanges, one on each side, to a central cylindrical support to prevent helium leak as shown in Figure 1. In this way, it creates an inner bath, which is considered isothermal in superfluid helium. Inside the central cylindrical support, a heater and an Allen Bradley (AB) temperature sensor are located and allow to apply heat and to measure the temperature of the inner bath. The description of the set-up is detailed in [6]. A capillary tube of 0.4-m length, carrying instrumentation wires is wrapped around the central support and insulated by Stycast® 2851 FT epoxy resin. Another AB temperature sensor is located in the cryostat bath, which is the temperature regulated. To achieve the temperature regulation of the cryostat bath, the pressure above the liquid surface is measured and held constant by a MKS Baratron® pressure sensor in combination with a pressure controller and a valve. The pressure sensor has an accuracy of ±0.25% of the reading and the pressure is controlled within ±0.02 Torr from 2.0 K to 1.4 K. Tests have been performed in saturated superfluid helium between 1.4 K and 2.0 K and thermometers are calibrated in situ before each experiment against the vapor pressure.

Five different thicknesses of Kapton HN have been tested that correspond to the DuPont gauges: 50 (12.7 μm), 100 (25.4 μm), 200 (50.8 μm), 300 (76.2 μm) and 500 (127 μm). The manufacturer gives thickness of the sheets with 20% accuracy, therefore the exact thickness has to be measured and these

values are presented in Table 1. The samples did not undergo any specific treatment except standard cleaning with alcohol.
The steady-state temperature measurement of the inner bath is obtained using a lock-in amplifier (SR850 Stanford Research Systems). The AB thermometer of the inner bath is placed in a series with a large resistance and the input feeding current is verified for each temperature. The temperature of the cryostat bath, T_b, is obtained with a four-wires technique and a DC battery current source. T_b is regulated within 1 mK and held constant for the entire range of power dissipation. The resulting temperature difference between the inner bath and the cryostat bath represents the overall thermal resistance of the Kapton sheets including the Kapitza resistance at the boundaries, the thermal resistance of the insulation due to conduction and heat leaks through the capillary as well as the stainless steel support.

3 Analysis principle

Although the Kapitza resistance depends strongly on the surface condition of the solid boundary with liquid helium, the acoustic mismatch theory can be used to predict the heat transfer mechanism to a great extent [7]. The heat transfer at the interface is seen as an energy exchange of phonons and their transmission through the He II-solid interface is governed by acoustics of continuous media. The thermal resistance results from the fact that not all the energy carried by the phonons can be transferred due to an acoustic mismatch between helium and solids. The heat flux, Q, going through the solid boundary is proportional to the difference in phonon energy density between the helium and solid material, which is proportional to $Q \propto T_s^4 - T_b^4$.
The Kapitza resistance at the surface of the sample in the inner bath, the resistance due to conduction, or the Kapitza resistance at the surface of the sample and the cryostat bath can all be used to define heat flux going through the sample Q_s. That is,

$$\frac{Q_s}{A} = \alpha(T_i^n - T_1^n) = \frac{\kappa}{\ell}(T_1 - T_2) = \alpha(T_2^n - T_b^n), \tag{1}$$

where A is the total cross section, *i.e.* the entire cross section of the two sheets, ℓ, the thickness of the Kapton sheets, κ, the average thermal conductivity of Kapton, n, the exponent of the power law and α the Kapitza coefficient. T_b and T_i are respectively the temperature of the cryostat bath and the inner bath, and T_1 and T_2 are the unknown boundary temperatures at the interface given by the Kapitza boundary conditions. The order of the Kapitza power law n, given by the mismatch theory is 4 but experimentally, the value is found to vary between 3 and 5 [8, 9]. In our data analysis we will keep n as a free parameter to compare our data with the theory. For temperature difference much smaller than the temperature of T_b or T_i, the Kapitza resistance on both side of the sample can be simplified to the first order as

$$\frac{Q_s}{A} = \alpha n T_i^{n-1}(T_i - T_1) = \frac{\kappa}{\ell}(T_1 - T_2) = \alpha n T_b^{n-1}(T_2 - T_b). \tag{2}$$

Taking $R = A.\Delta T/Q$ as the definition for thermal resistance, where ΔT stands for any temperature difference in a given medium, the thermal resistance of the sample, R_s, which is the sum of the two Kapitza resistances at the helium boundary and the resistance due to thermal conduction in the sheet, becomes

$$R_s = \frac{1}{\alpha n T_i^{n-1}} + \frac{\ell}{\kappa} + \frac{1}{\alpha n T_b^{n-1}}. \quad (3)$$

Note that R_s is a function of the inner and cryostat bath temperatures and the thickness of the Kapton sheet. Equation (3) can be simplified by linearization to give

$$R_s = \frac{2}{\alpha n T_b^{n-1}}\left(1 - \frac{1}{2}\frac{\Delta T}{T_b} + O(\Delta T)^2\right) + \frac{\ell}{\kappa} \approx \frac{2}{n\alpha} T_b^{1-n} + \frac{\ell}{\kappa}. \quad (4)$$

where ΔT is the total temperature difference across the sheets, $\Delta T = T_i - T_b$. Note that the second term of left end side of Equation (4) corresponds to 0.5% to 0.7% of the total resistance value in our experiment and will be neglected hereafter for simplicity. The first term of the right end side of Equation (4) is the Kapitza resistance whereas the second term is due to conduction.

4 Error Analysis

4.1 Heat Losses

The total heat flux dissipated by the heater is $Q = Q_s + Q_{cap} + Q_{sup}$ where Q_s is the heat flux through the Kapton sheets while Q_{cap} and Q_{sup} are respectively heat losses via the capillary and the stainless steel support. Q_{cap} and Q_{sup} constitute systematic errors in the evaluation of Q_s. To estimate Q_{sup}, the experimental set-up has been modeled with a finite element analysis [6]. Results show that the heat flux through the sample and the stainless steel support can be considered as parallel conductors and this loss represents 2% of the total heat flux through a Kapton 100 HN sheet at 1.9 K, for example, over the entire range of Q (maximum value of 150 mW reached for 500 HN sample). The second type of heat loss is through the helium contained in the capillary. The capillary contains 6×120µm-diameter copper wires and 4×100µm-diameter superconducting wires. Its cross-sectional area is 0.157 mm^2. The equivalent cross-section of the capillary is estimated to be 5.83 10^{-2} mm^2. This heat loss can reach up to 20% of the total heat flux for ΔT<1 mK. To avoid such high heat loss and to be in the $\Delta T \ll T$ condition, we limit the data reduction of ΔT in the temperature range of [10-30 mK] where the loss is comprised between 2.5% and 1.5% of the total heat flux for the same example. The heat flux density is always smaller than 30 W/m^2. Calculations of heat losses are considered as estimation with an uncertainty of 20%, and the uncertainty on these calculations are included in the error analysis accordingly.

4.2 Experimental errors

The lock-in amplifier, used for temperature measurement, is connected to the power network through an insulation transformer in order to minimize electrical disturbances. The AB thermometer is placed in series with a 5 MΩ stable resistance at room temperature. The lock-in amplifier provides an AC voltage of 5 V rms at 5 Hz across the two resistances to obtain a feeding current through the AB thermometer of 1µA within 0.2%. The feeding current is measured for each run. The electronic chain provides temperature measurement sensitivity between ±20 µK at 1.4 K and ±200 µK at 2.0 K. The Temperature difference error is at most 0.2 mK in the range of our investigation. This error analysis includes the resistance error measurement and the propagation error through the calibration curve. Total heat flux, is generated and monitored by a Keithley 2400 source meter and uncertainty is at most 0.5% of the value.

4.3 Fitting procedure

In order to extract simultaneously the thermal conductivity and the Kapitza resistance values as a function of temperature, different thicknesses of the same material at different bath temperature must be tested. The first step is to extract the total resistance of the sample R_s. Figure 2 presents a typical curve of the total temperature difference, ΔT, across a Kapton 100 HN sheet versus the heat flux through the sample Q_s. These results show the expected trend; that is the overall thermal resistance rises with decreasing temperature because the Kapitza resistance is proportional to T^{-n} (with n>0) and the thermal conductivity of Kapton increases with temperature. The thermal resistance of the sample, R_s, is determined by a linear least square method. The Figure 2 exhibits the uncertainties in ΔT, which includes the inherent uncertainty of the measurement, $\sigma_{\Delta T}$, and the uncertainty due to variations in Q_s corresponding to the uncertainty in the measurement, σ_{Qs}. This indirect contribution, $\sigma_{\Delta T}(Q_s)$, is taken into account because it is of the same order of magnitude or sometimes larger than $\sigma_{\Delta T}$. It can be approximated to the first order by,

$$\sigma_{\Delta T}(Q_s) \approx \sigma_{Q_s} \frac{d\Delta T}{dQ_s}. \tag{5}$$

The total uncertainty of ΔT is constructed as a quadratic sum of $\sigma_{\Delta T}$ and $\sigma_{\Delta T}(Q_s)$ [10]. Figure 3 represents the thermal resistance of the samples as a function of thickness for 1.9 K. For each bath temperature, such curve is created and the data are fitted with the second part of Equation (4) with a non-linear least square method where the independent variable is the thickness, ℓ and the dependent variable is the thermal resistance, R_s. The uncertainty of thermal resistance presented in this plot includes the uncertainties due to the fitting of the raw data and the ones from the determination of the cross-section of the sample.

5 Results and discussion

5.1 Thermal resistance

Figure 4 presents the thermal resistance, R_s, for all the Kapton sheets tested as a function of the temperature. Typically for the 50 HN Kapton sheet the uncertainty represents roughly 10% of the value whereas for the 500 HN Kapton it is comprised from 1% to 3%. The influence of the thermal resistance due to conduction is clearly seen in Figure 4 where the total thermal resistance of the sample increases with the thickness for a constant bath temperature. One can show also by fitting the data with $a+b/T^n$ that its evolution with temperature becomes progressively non-linear as the thickness decreases due to the growing influence of the non-linear Kapitza resistance.
To extract the thermal conductivity and the Kapitza resistance, R_s is plotted as a function of the thickness of the sheet for each temperature, as shown in Figure 3 for 1.9 K. The uncertainty of the thermal conductivity is around 3% for all samples and for the thermal resistance it varies between 13% at 2.0 K and 9% at 1.4 K. This difference is due to the fact that the thermal conductivity corresponds to the inverse of the slope, which is not sensitive to error bars associated to the total thermal resistance, whereas the Kapitza resistance, which corresponds to the value at null thickness, is extremely sensitive.

5.2 Thermal conductivity

At low temperatures, the thermal conductivity of amorphous polymer is known to exhibit a quadratic dependency with temperature ($\kappa \propto T^2$) below 1 K and for higher temperature range (5 K to 15 K) a

plateau is reached [11]. Between these two regions, one expects that the temperature dependency of the thermal conductivity to follow a power law T^n with n between 0 and 2. In our measurement, we found κ to be linearly dependent on temperature. It is thus consistent with the above prediction and the magnitude is in good agreement with recent results reported by other authors [3, 4]. As our temperature range of investigation is small and to comply with theoretically temperature dependency, we propose a linear evolution as,

$$\kappa=[(2.28\pm0.54)+(2.40\pm0.32)\times T]\times 10^{-3} \quad \mathrm{Wm^{-1}K^{-1}} \tag{6}$$

In Figure 5, κ is presented and compared to other data in literature. Our results are in the same order of magnitude to the results presented by other groups employing very different approach to determine κ. Our value is even comparable to the value found by Lawrence *et al.*, by $\kappa=4.638\ 10^{-3}\times T^{0.5678}\ \mathrm{Wm^{-1}K^{-1}}$, which is the most recent data determined through the stack method. In their experiment, the thermal conductivity of Kapton HN was determined, in the range of 0.5–5 K, with two different stacks. This two-stack method, as it is called, allows extracting the Kapton thermal conductivity without evaluating the thermal conductivity of the epoxy resin and the thermal contact resistance. The stacks they used were composed with two different numbers of sheet, 100 and 200, with two different Kapton sheet thicknesses, 25 μm and 125 μm, respectively. κ found here is smaller by a factor of two to the data presented by Barucci *et al*, which follow $\kappa=(6.5 \pm 0.2)\ 10^{-3}\times T^{1\pm0.02}\ \mathrm{Wm^{-1}K^{-1}}$ in the range of 0.2–5 K.

5.3 Kapitza Resistance

The best fit to the Kapitza resistance data is shown in Figure 6 and can be described as,

$$R_K=[(8538\pm1594)\ T^{-(2.57\pm0.35)}]\times10^{-6} \quad \mathrm{Km^2W^{-1}} \tag{7}$$

The observed non-linear law ($R_K \propto T^{-2.57}$) in our results is consistent with the theory discussed above. Here, the Kapitza coefficient, α, defined in Equation (4), is given as $\alpha=65.51\pm19.0\ \mathrm{Wm^{-2}K^{-3.57}}$. The dependency of the two fitting parameters in Equation (7) is very high suggesting that the fitting law is over parameterized. Therefore, the uncertainty of these two parameters should not be viewed simply as errors but more correctly as variations due to the other fitting parameter. Thus we choose to fit the data by the law imposed by the theory. The result gives

$$R_K=(10540\pm444)\ T^{-3}\times10^{-6} \quad \mathrm{Km^2W^{-1}} \tag{8}$$

This is also depicted in Figure 6 as a dotted line. From this expression, one can deduce the Kapitza coefficient as $\alpha=47.43\pm2.00\ \mathrm{Wm^{-2}K^{-4}}$. Our R_K values are an order of magnitude higher than Nacher's result, which follows a power law $R_K=0.7\ T^{-3}\times10^{-3}\ \mathrm{Km^2W^{-1}}$ in the range of their investigation. Granted that their analysis was done with an infinite thermal conductivity for the Kapton sheet, we remark that their finding is still perplexing considering that the small value of the thermal conductivity will force the second term in Equation (4) to be negligible within their range of investigation. It should also be noted that they do not offer any viable explanation why their value is an order of magnitude lower than the value of Kapitza resistance between liquid helium and solids, except by a possible thermal leak. The facts that our thermal conductivity value is in the same order of magnitude with other results, that our Kapitza resistance is typical for solid-He II interface and that it is in close agreement with the theoretical model make us confident of our results.

6 Conclusion

The thermal conductivity reported here is comparable to those found in the literature with good accuracy. For small ΔT, the determined Kapitza resistance is within 10% of the theoretical cubic temperature dependency and is in the order of Kapitza resistance of solid-He II interface. The method, that determines simultaneously the Kapitza resistance and the thermal conductivity, gives results with good accuracy for Kapton foils and could be used for other polymers used in cryogenic environment.

Acknowledgments

The author is grateful to S. Carré and E. Bourlot for technical help and to Dr. Nakamae for helpful discussion.

References

[1] Yokoyama H. Thermal conductivity of polyimide film at cryogenic temperature. Cryogenics 1995; 35: 799-800.

[2] Benford DJ, Powers TJ, and Moseley SH. Thermal conductivity of Kapton tape. Cryogenics 1999; 39: 93-95.

[3] Lawrence J, Patel AB, and Brisson JG. The thermal conductivity of Kapton HN between 0.5 and 5 K. Cryogenics 2000; 40: 203-207.

[4] Barucci M, Gottardi E, Peroni I, and Ventura G. Low temperature thermal conductivity of Kapton and Upilex. Cryogenics 2000; 40: 145-147.

[5] Nacher PJ, Schleger P, Shinkoda I, and Hardy WN. Heat exchange in liquid helium through thin plastic foils. Cryogenics 1992; 32: 353-361.

[6] Baudouy B, François MX, Juster F-P, and Meuris C. He II heat transfer through superconducting cables electrical insulation. Cryogenics 2000; 40: 127-136.

[7] Khalatnikov IM. An introduction to theory of superfluidity. New York Amsterdam: Benjamin Publishing inc., 1965.

[8] Snyder NS. Heat transport through helium II : Kapitza conductance. Cryogenics 1970; 10: 89.

[9] Challis LJ. Kapitza resistance and acoustic transmission across boundaries at high frequencies. Journal of Physics, C, Solid State 1974; 7: 481.

[10] Bevington PR and Robinson DK. Data reduction and error analysis for the physical sciences. 2nd ed: WCB McGraw-Hill, 1992.

[11] Hartwig G. Polymer Properties at room and cryogenic temperature. New York: Plenum Press, 1994.

Table 1. Description of Kapton tapes

	ℓ, Thickness (μm)	A, Cross section (mm^2)
50 HN	14±1	8938 ± 136
100 HN	25±2	8581 ± 132
200 HN	53±1	9026 ± 149
300 HN	76.8±1.3	8671 ± 137
500 HN	128.4±1.7	8940 ± 103

List of Figures

Cryogenics, Baudouy, Figure 1

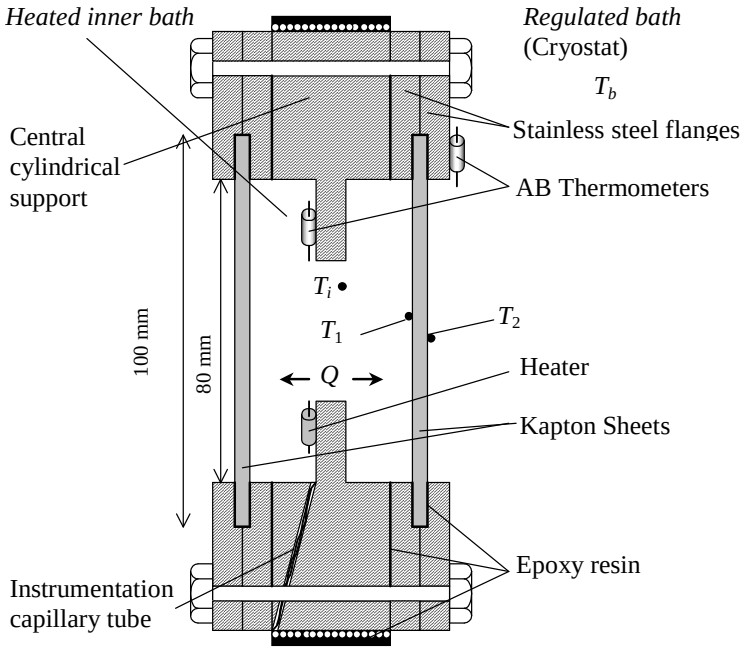

Cryogenics, Baudouy, Figure 2.

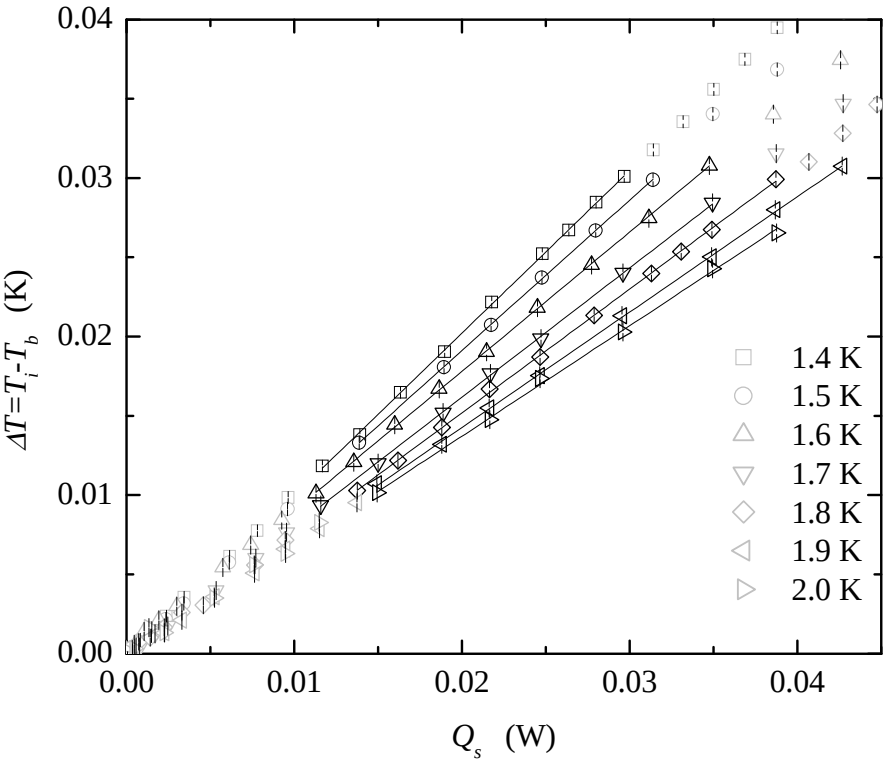

Cryogenics, Baudouy, Figure 3

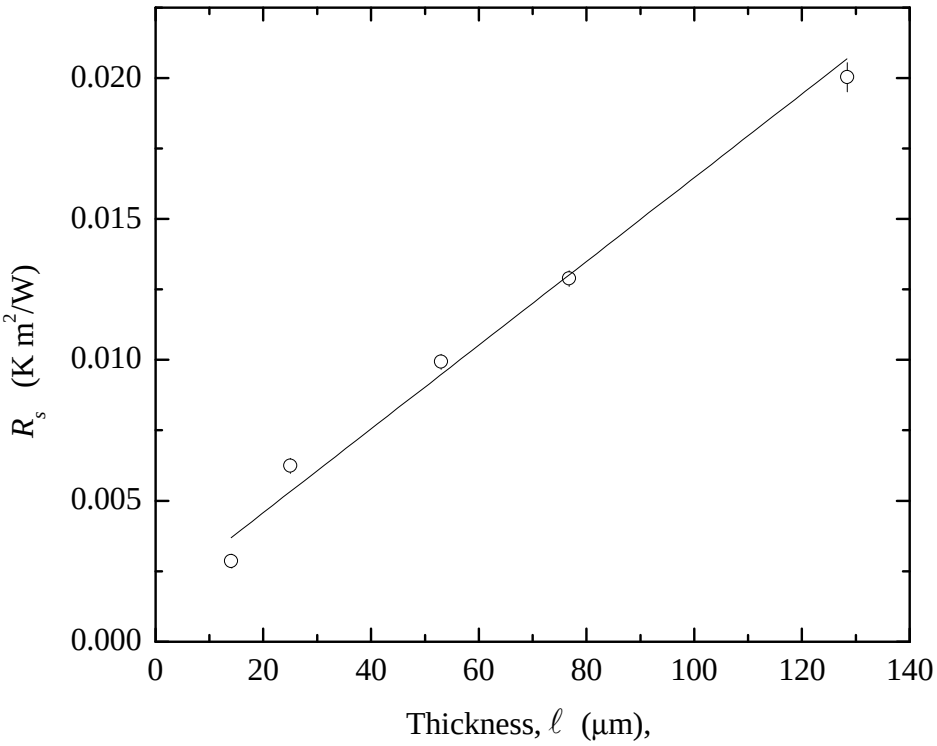

Cryogenics, Baudouy, Figure 4

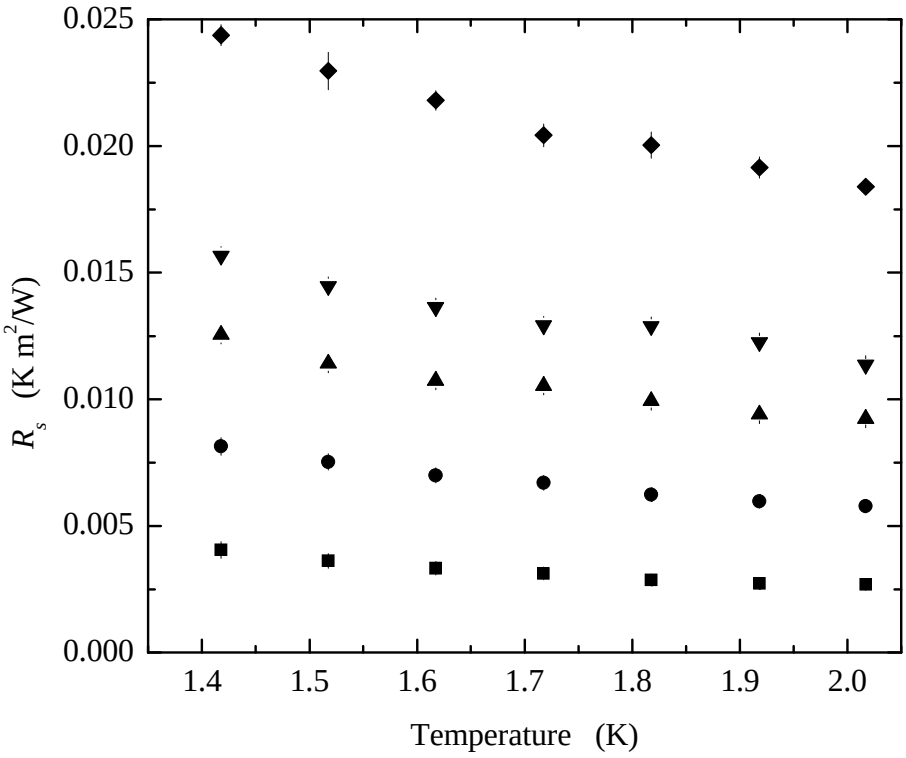

Cryogenics, Baudouy, Figure 5

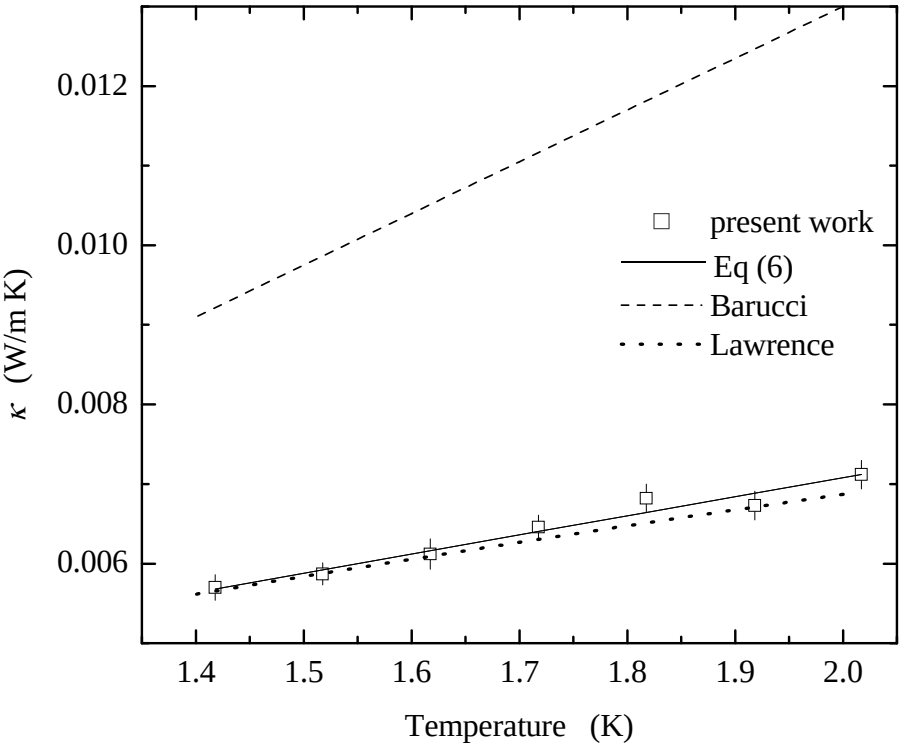

Cryogenics, Baudouy, Figure 6